Proceedings of the 11th Brazilian Congress of Thermal Sciences and Engineering -- ENCIT 2006
Braz. Soc. of Mechanical Sciences and Engineering -- ABCM, Curitiba, Brazil,- Dec. 5-8, 2006

Paper CIT06-0799

EXPERIMENTAL STUDY OF HORIZONTAL PLUG FLOW BY ULTRASONIC AND VISUALIZATION TECHNIQUES

J.L.H. Faccini, P.A.B. Sampaio
Instituto de Engenharia Nuclear - IEN / CNEN
CP 68.550, 21945-970, Rio de Janeiro, Brazil
faccini@ien.gov.br, sampaio@ien.gov.br

J. Su
Nuclear Engineering Program, COPPE
Universidade Federal do Rio de Janeiro
CP 68.509, 21945-970, Rio de Janeiro, Brasil
sujian@con.ufrj.br

Abstract. *This work presents an experimental study of intermittent elongated bubbles typical of horizontal plug flows. Bubbles of different shapes and velocities were identified by a hybrid time averaging ultrasonic and high-speed motion visualization techniques. The hybrid ultrasonic technique determines the liquid film thickness under the elongated bubble and liquid plug velocity. The liquid film thickness is obtained by measuring the transit time of an ultrasonic pulse discharged from a single transducer, reflected by the bubble gas-liquid interface and received by the same transducer. The liquid plug velocity is determined by indirect acoustic transmission discharged through the entirely flow cross section by an emitter transducer, reflected by the tube wall and received by a receiver transducer. The high-speed visualization allows to observe the bubble shape and to measure their velocities.*

Keywords*. elongated bubble, plug flow, bubble velocity, two-phase flow, horizontal flow.*

1. Introduction

In a PWR nuclear power plant undesirable situations may occur when the coolant does not flow as single-phase liquid but instead, complex two-phase mixture may arise into the reactor core and primary circuit. The problem becomes more severe when the pipe is horizontal, because the flow varies considerably over the cross section due to its fluctuating nature. Thus, even when the mixture flowrate is maintained at a steady value, the component mass flow rates, phase velocities and pressure at any cross section normal to the pipe axis may exhibit variations with respect to time much larger than those found in single-phase flow. As a result, processes such heat and mass transfer are unsteady, with substantial variation of the system temperature and concentration profiles occurring. Other potential consequences include increased erosion-corrosion of the pipe and the onset of damaging resonant vibrations within the systems. Consequently, an understanding of the coolant two-phase flow is extremely important from the point of view of nuclear reactor engineering, to produce the most effective equipment design and to obtain accurate predictions of system properties.

In horizontal flow pattern maps, the plug flow regime exists over a wide range of gas and liquid flow rates (Mandhane et al., 1974; Taitel and Dukler, 1976). It is high complex, inherently unsteady, and generally described in literature as a sequence of liquid plug zone containing dispersed few small bubbles, followed by an elongated bubble over a non-uniform thin liquid film (Collier, 1981; Wallis, 1969 and Whalley, 1996).

The theoretical models to predict the plug flow parameters have been developed in the last decades based on the unit cell concept proposed by Wallis (1969) and more recently on a statistical cell unit approach by Fabre and Liné (1992). Although these models are capable to predict important flow parameters such as pressure gradient, average phase velocities and void fractions, they are not able to predict the flow structure itself, i.e., the elongated bubble local velocity and length, and its evolution along the tube. The experimental measurement of plug flow is a specialized matter that requires careful experimentation and appropriate techniques. The main requirement of a measurement technique to be successful for a horizontal plug flow is to have a high degree of spatial resolution, as the flow varies considerably over the cross section. The ultrasonic techniques have been proved to be one of the most reliable methods for two-phase flow measurements, offering more practical applications and can be used when other alternative methods are not available (Chang et al., 1982; Chang and Morala, 1990). Faccini et al. (2004) have proposed a contra-propagating transmission ultrasonic technique to identify plug flow regime and to measure the average void fraction in horizontal air-water two-phase flow. The plug regime was recognized by the analysis of histogram bars of the ultrasonic flow rates readings and it was possible to calculate the liquid volumetric fraction from the air-water flow rate fluctuations. Recently, Masala et al. (2005) developed a high-speed, four transducers, pulse-echo ultrasonic technique for the measurement of interfacial parameters of horizontal two-phase plug flow. The lengths and velocities of liquid plugs and elongated bubbles were determined by tracking one of the edges of the plugs using two ultrasonic transducers, and a new experimental correlation was proposed.

Flow visualization is another experimental technique that has become a powerful tool to study the two-phase flow providing valuable information on the void fraction, flow pattern, gas and liquid velocities (Dinh and Choi, 1999 and Zaruba et al., 2005). When applied to horizontal plug flow, it is possible to extract information on the elongated bubble structure such as the bubble nose and tail evolution, length and velocity (Fagundes Netto, 1999).

In this work, we combined a hybrid type ultrasonic technique for flow and void fraction measurements with a visualization technique for bubble velocity measurements in horizontal plug flow, which was applied in a two-phase air-water test section at the experimental thermalhydraulics laboratory of the Nuclear Engineering Institute (IEN/CNEN), Rio de Janeiro. The liquid flow rate measurements were used to determine the average void fraction, liquid hold up and liquid-phase velocities. The results obtained are presented in comparison with available correlations from literature. The results of the liquid film thickness measurements for different gas-liquid flow rates are also presented. From the images taken with a visualization system, a series of individual elongated bubbles were tracked and their nose and tail velocities were estimated by using an acquisition and image analysis program. These results are compared with some correlations published in the literature.

2. Experimental setup

2.1. Two-phase flow test section

The two-phase test section used in this work consists of a venturi mixer, a horizontal tube, an expansion reservoir and an air water separation tank as shown in Fig. 1. The horizontal tube is a 6 m long stainless steel AISI316 with an inner diameter of 0.0512 m, followed by a short tube 0.6 m long transparent extruded acrylic with the same inner diameter. Distilled water is circulated axially through the venturi mixer, coming from an existing single-phase water loop which is equipped with a centrifugal pump and a metering rig. Air is injected radially into the mixer by a compressor through a flow line equipped with appropriate air instrumentation. The air-water mixture goes out from the mixer and travels through the stainless steel tube along its length until the transparent acrylic tube where it can be observed visually. The air and water flow rates are measured by turbine flowmeters in single-phase conditions. The air-water two-phase flow is monitored by a hybrid contrapropagating transmission ultrasonic flowmeter – pulse-echo ultrasonic liquid film thickness measuring system.

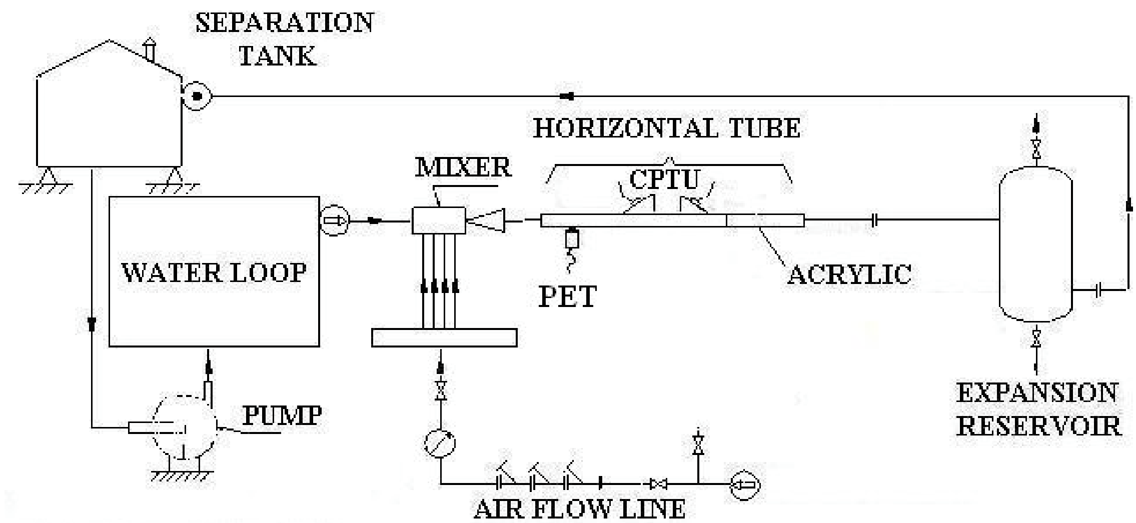

Figure 1. Schematic of the two-phase test section.

2.2. Ultrasonic and visualization systems

The ultrasonic system is formed by an industrial contrapropagating transmission ultrasonic flowmeter (CPTU) with a FieldBus data acquisition unit; a pulse-echo ultrasonic transducer (PET) 10 MHz and 13 mm diameter with pulser receiver, digital oscilloscope and a PXI computer based on LabView platform. The CPTU flowmeter has two transducers attached to the outside wall of the stainless steel horizontal tube, next to the transparent acrylic tube, placed respectively upstream and downstream on the same sides and tilted of 45 degrees as shown in Fig. 2. Each one transducer alternatively transmits and receives an ultrasonic signal, which is reflected by the tube wall (V-path). The difference in the transit time between the pair of the transducers can be measured and used to calculate the water volumetric flow rate with 1% of accuracy (Ultraflux, 1998).

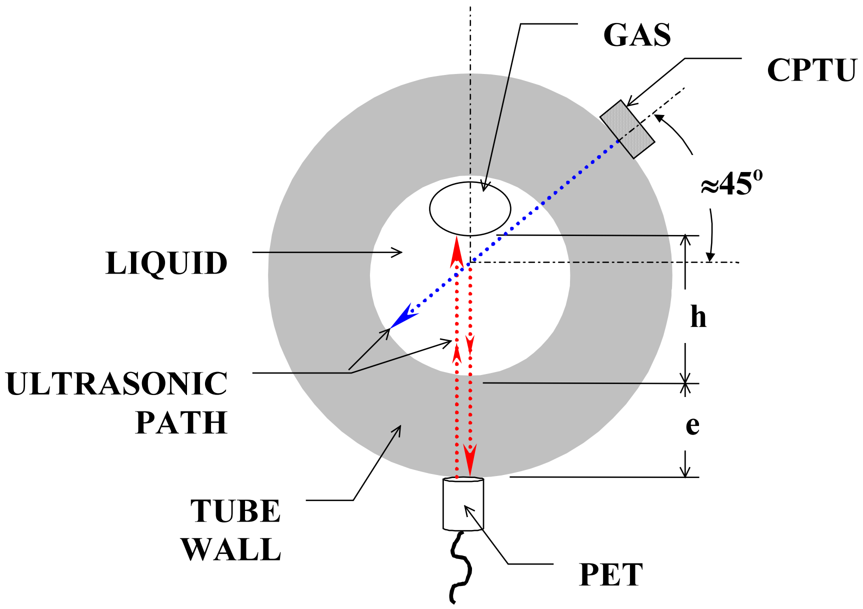

Figure 2. Cross-sectional view of gas-liquid plug flow in a horizontal tube with CPTU and PET instrumentation.

For the PET system, the ultrasonic transducer was placed at the bottom of the stainless steel tube section next to CPTU system for liquid film thickness as is shown in the Fig. 2. A part of ultrasound pulse in pulse-echo mode discharged from the emitter-receiver transducer, placed at bottom of tube, is transmitted through the water and then reflected back to the same transducer from air-water or tube wall-water interfaces. These signals are acquired by an oscilloscope over a period of time and then plotted as the waveforms. Figure 3 shows waveforms corresponding to air-water plug flow through the horizontal tube, where the reflected pulses can be divided in two sets: initial (I), wall-liquid (WL) and liquid-gas (LG) are corresponding to the liquid film region; liquid-wall (LW) and wall-gas (WG) are corresponding to the liquid plug region. For ultrasonic signals in the 10 MHz range the attenuation in the wall, water film and at their interfaces is small compared to that in the air. This phenomenon can be explained by the theory of sound due to the great difference in characteristic acoustic impedance between the air and the water resulting in a high reflection factor. All reflected signals are received by the same PET transducer and handled by the pulser-receiver. The output signals are digitilized on the digital oscilloscope which is controlled by a GPIB interface, and stored in the computer hard disk for more detailed analysis afterwards. The measurement of the liquid-gas interface height was carried out by recording 50 ultrasonic waveforms per run provided by the oscilloscope at an acquisition time interval of 1 s. Each waveform acquired was formed by 10,000 points. A computational algorithm was written to examine the digitilized signals, and from them, to identify the maximum peaks corresponding to each reflected pulses set. By measuring the transit time between WL maximum pulse peak and LG (and LW) maximum pulse peak, the liquid film height and the liquid plug height can be determined, provided that the sound velocity in water is known. In all these experiments the sound velocity value was 1497 m/s.

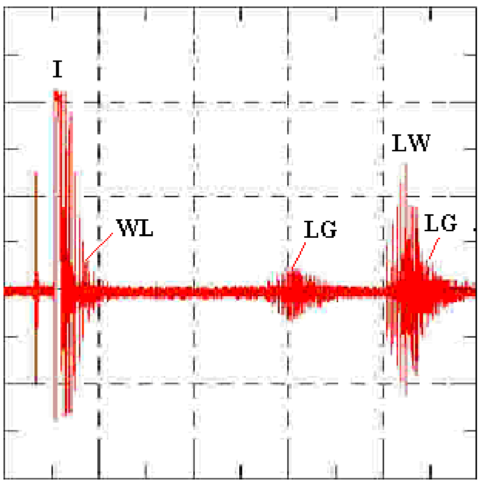

Figure 3. Typical ultrasonic signals for a plug flow with Q_{Ls} = 6,0 m^3/h and Q_{Gs} = 1,0 m^3/h.

The visualization system is formed by a monochrome digital high-speed camera, shown in Fig. 4, which is, equipped with a CCD sensor (maximum resolution 480 x 420 pixels), zoom lenses, a PCI controller board of 12 bits, an acquisition & image analysis program, and a computer. Tripods and mounting devices complete the system, which has capacity to record sequences of black & white images from 50 to 8000 frames per second. The camera was positioned after the PET system at a distance larger than10 times the horizontal tube inside diameter. Complete control of the camera operating system including frame rate triggering, adjustment image resolutions and shutter speed was carried out through the personal computer. The professional zoom objective lens of the camera could be focused at distances shorter than 1.0 m. The lightning system includes a light projector placed in front of and above the acrylic tube. Positioning was important for preventing shadowing and reflections and for ensuring good image quality. For each frame rate only a set of pre-determined spatial resolutions are available. Higher spatial resolutions result in longer recording times and fewer video frames per unit time, so that a compromise between speed and resolution has to be made. The frequency range from 125 to 250 frames per second was found to be adequate for the measurements and was used in all experiments reported in this paper. The camera recording was started and stopped manually when the last 5 ultrasonic waveforms have to be recorded. The sequence of images displayed on the computer monitor could be stored in a computer file, retrieved and replayed to analyze the flow motion sequence in detail. The set of discrete pictures were saved as a series of 512 greyscale avi images with a spatial resolution of 480 × 420 pixels. The information on the elongated bubble motion within the tube was obtained by processing about 5000 frames. A position reference can be superimposed on the images stored in the computer file. A horizontal and a vertical lines that intersect at a target provide X and Y coordinates, as can be seen in Fig. 5. This feature could be used to determine distances between two points in the picture. The system was calibrated by measuring the physical distance between two points of interest on the rule and entering the distance between the set points in the system. The system then calculates the distance between any two points on the monitor. If the points are on different frames, the system also calculates the velocity of the point of interest. All measurements are in two dimensions perpendicular to the camera.

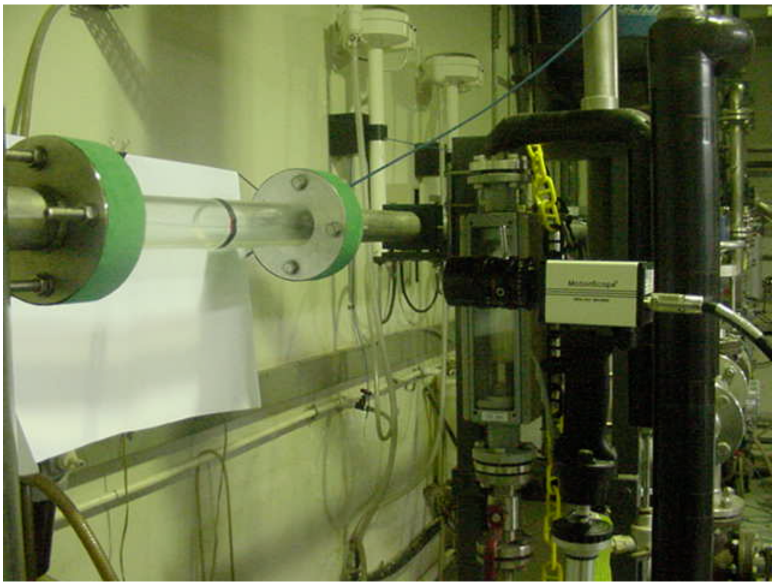

Figure 4. Photographic view of visualization system.

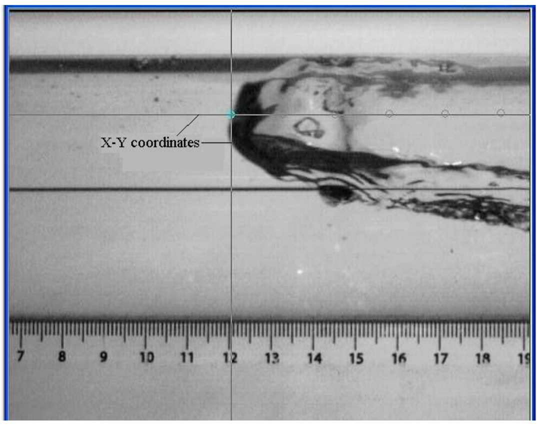

Figure 5. The X-Y coordinates to visualization system.

3. Liquid-phase and liquid film measurements

The water volumetric flow rate was determined by the product of the cross-sectional area of the tube and the liquid mean axial velocity. This implies that the water volumetric flow rate given by the CPTU flowmeter includes both liquid film and liquid plug flow rates. We made the assumptions that the flow is fully developed, the flow profile correction coefficient is the same for single-phase flow, and the liquid mean axial velocity is at the center of flow tube. In the experiments the water single-phase flow rate was determined by a turbine flowmeter with 0.5% of estimated accuracy; as the air flow rate starts to increase the CPTU flowmeter measures the water phase flow rate travelling together with air inside the tube. We can determine the liquid hold up of the air-water mixture dividing the water single-phase flow rate by the current water two-phase flow rate, then the liquid hold up can be obtained by the relation:

$$(1\text{-}\alpha)=\frac{Q_{Ls}}{Q_L} \tag{1}$$

where α is the void fraction, Q_{Ls} is the single-phase volumetric liquid flow rate and Q_L is the two-phase volumetric liquid flow rate. The local average liquid phase velocity U_L can be calculated by:

$$U_L=\frac{Q_L}{A} \tag{2}$$

where A is the whole cross-sectional area of the tube.

Measuring the transit time of the ultrasound pulse and knowing the sound velocity through water, the water film thickness under an elongated bubble h_L can be calculated by the relation:

$$h_L=c_w\,\frac{\Delta t}{2} \tag{3}$$

where c_w is the water sound velocity at a given temperature and Δt is the ultrasound transit time.

Figures 6(a) and 6 (b) show typical pictures of a plug regime taken with a high-speed camera, where an elongated bubble moves from the right to the left in a horizontal tube, for the same gas flow rate and two different liquid flow rates. It can be observed in Figs. 6 (a, b) that the elongated bubble propagates in the upper part of the tube with a liquid film thickness under it varying along its length, and a roughly interface between them. While the average liquid plug velocity and dispersed bubbles velocity are not necessarily the same, the elongated bubble propagates with a translational velocity different from that of the liquid film which vary along the pipe due the variation of the film thickness.

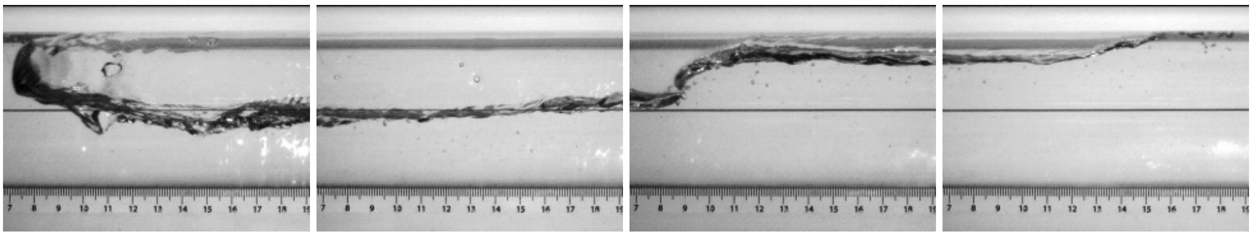

(a)

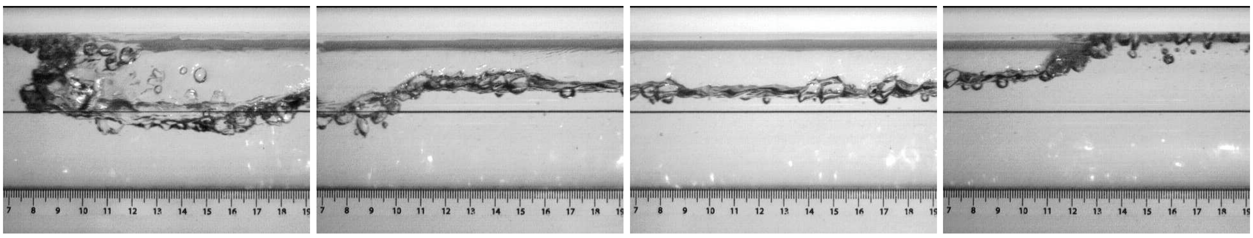

(b)

Figure 6. An elongated bubble moving in a horizontal tube: a) Q_{Ls} = 6,0 m^3/h and Q_{Gs} = 1,0 m^3/h; b) Q_{Ls} = 10,0 m^3/h and Q_{Gs} = 1,0 m^3/h.

Figures 7 and 8 show typical liquid level measurements obtained with PET ultrasonic transducer mounted at the bottom side of the circular tube of the test section for plug flow. Two cases with different superficial liquid flow rates for the same superficial gas flow rate are presented. It can be observed that the liquid level fluctuates between a minimum and a maximum that correspond respectively to ultrasonic signals reflections in the liquid-gas interface under an elongated bubble moving in front of the transducer, and to reflections in the tube wall through the liquid plug coming soon after. Another features observed are the minimum value fluctuations which indicate that the liquid-gas interface is not smooth, as can also be seen from the pictures shown in Fig. 6.

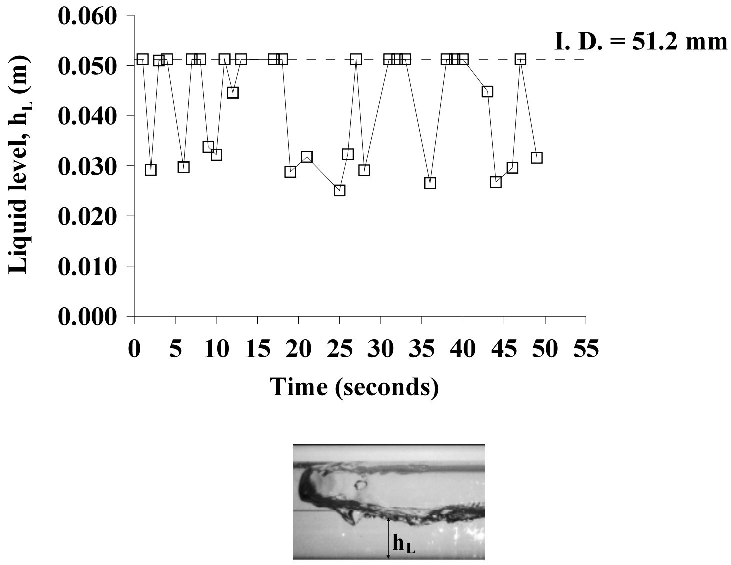

Figure 7. Time averaged liquid level for Q_{Ls} = 6.0 m^3/h and $Q_{G\,s}$ = 1.0 m^3/h.

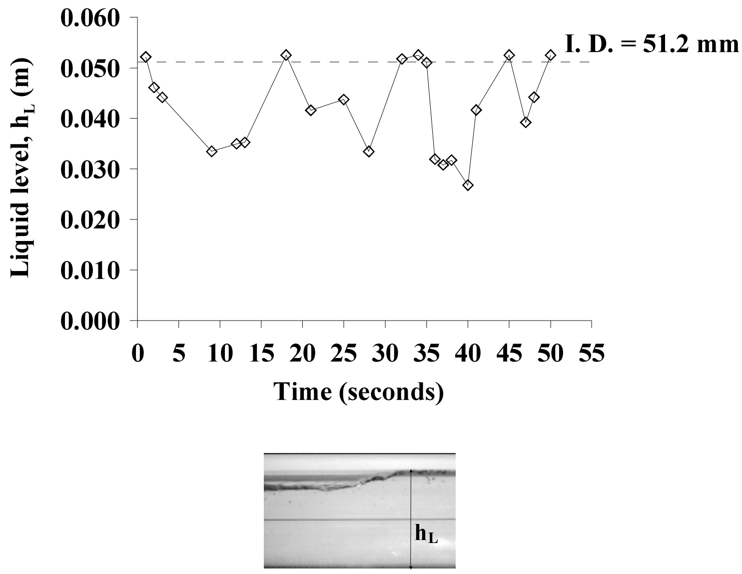

Figure 8. Time averaged liquid level for Q_{Ls} = 10.0 m^3/h and $Q_{G\,s}$ = 1.0 m^3/h.

Figures 9 and 10 show the void fraction and liquid hold up estimated in terms of air-water flow rates measured by CPTU for different air flow rates and the superficial water flow rate measured by the turbine flowmeter as explained previously. In Fig. 9 the void fraction estimated results are compared with the correlation of Wallis (1969), and can be observed that the approach to determine the water velocity applying the Eq. (2), taking into account the distance between transducers determined as if the water is flowing alone, has given water velocity values strongly influenced by the hypothesis made with great discrepancies to expected values from Wallis correlation. This approach is under review. In Fig. 10 the liquid hold up results are compared with the generalised correlation after Beggs and Brill (1973).

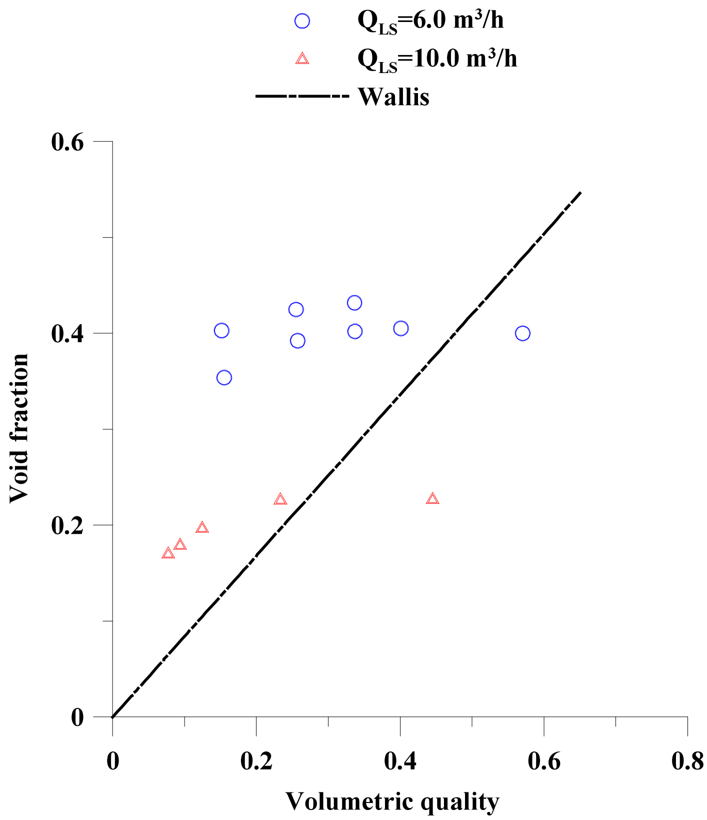

Figure 9. Void fraction estimated from CPTU measurements as a function of volumetric quality.

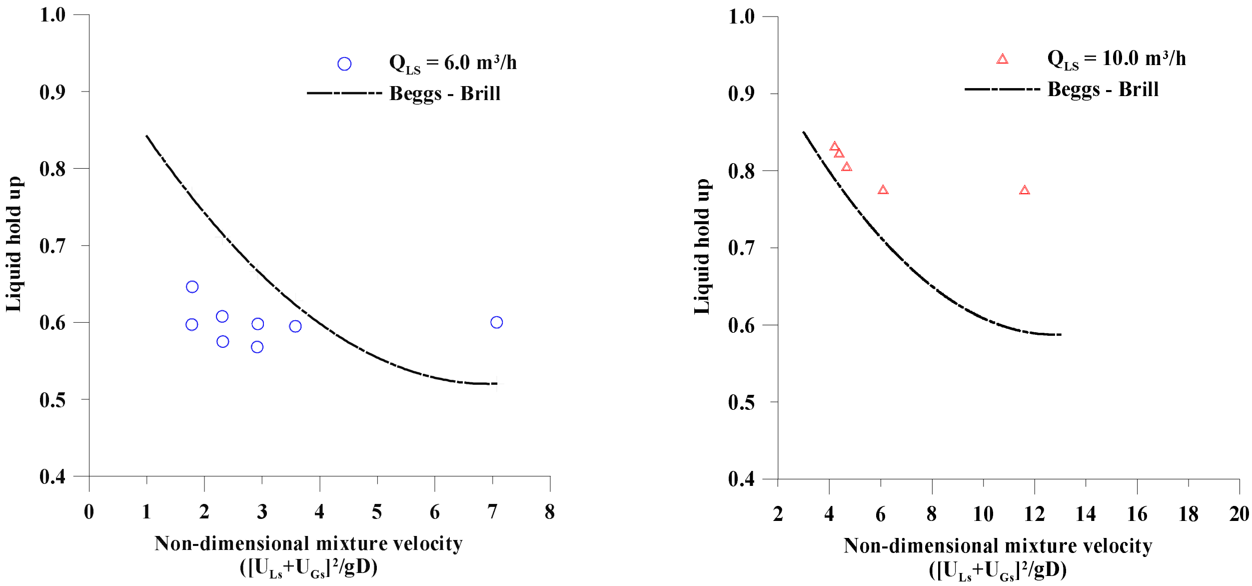

Figure 10. Liquid hold up estimated from CPTU measurements for Q_{Ls}=6.0 m^3/h and 10.0 m^3/h as a function of mixture velocity.

4. Bubble nose and tail velocity measurements

In this section the bubble nose and tail velocity measurement results are presented over about 5,000 frames analyzed as explained in section 2.2. The directly measured bubble nose and tail velocities are shown in Fig. 11 for two liquid flow rates and six gas flow rates. It can be seen that the nose and tail velocities differ in some cases more than expected. A possible explanation to the data deviation from the equal velocities line is the presence of non-stable bubbles accelerating and decelerating during their resident time into transparent section. Also, the difficulty to track the nose or the tail along the frame sequences due to shadowing and light refraction effects may introduce a bias in the bubble velocity measurements.

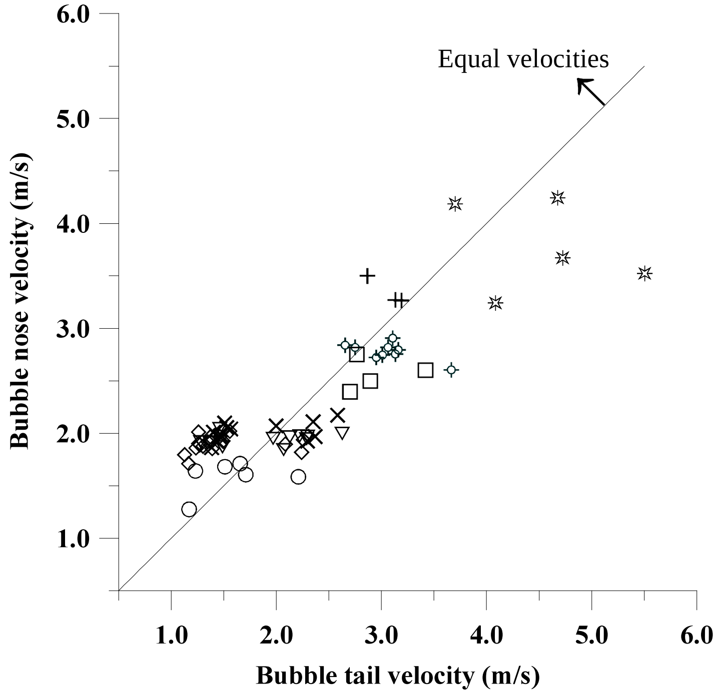

Figure 11 . Measured bubble nose and tail velocity.

Figure 12 shows the bubble velocity versus the local liquid velocity given by the Eq. (2) in the non-dimensional form. A fit to the classic model of Nicklin et al. (1962) with the experimental correlation obtained by Bendiksen (1984) was attempted.

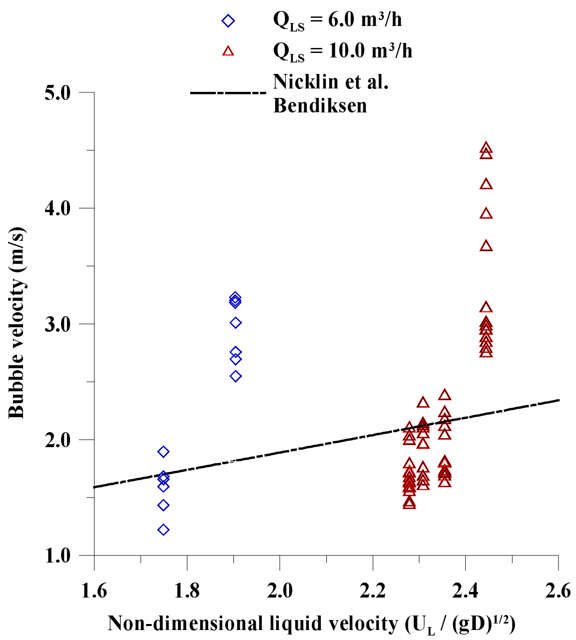

Figure 12. Bubble average velocity as a function of liquid velocity. Comparison with Nicklin et al. model and Bendiksen correlation.

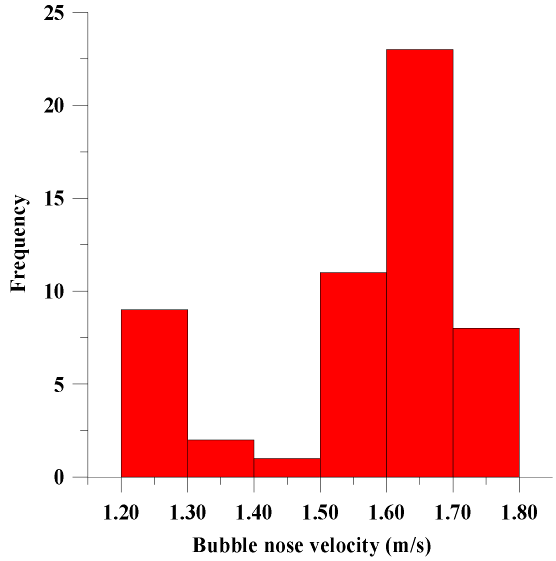

(a)

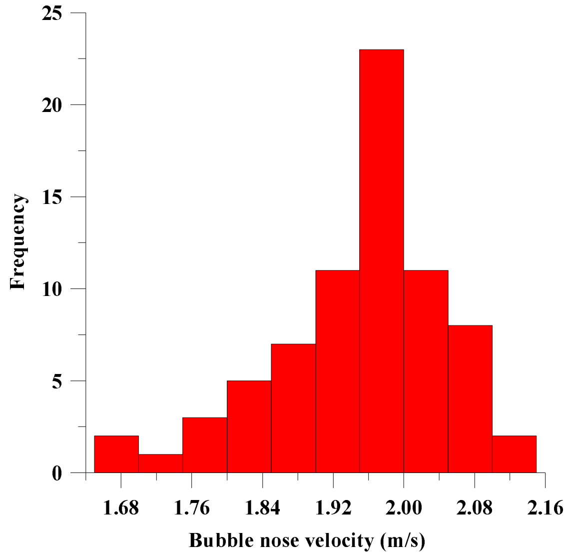

(b)

Figure 13. Histograms for bubble nose velocity distribution in plug flow: a) Q_{Ls} = 6,0 m^3/h e Q_{Gs} = 1,0 m^3/h; b) Q_{Ls} = 10,0 m^3/h e Q_{Gs} = 1,0 m^3/h.

Fig. 13 illustrates the difficulties to determine the elongated bubble velocity in a horizontal plug flow. The histograms presented are related to the pictures showed in Fig. 6 on which the elongated bubble nose velocities were measured by tracking them along an image sequence. The results denote the fluctuating nature of this regime.

5. Conclusions

In this paper, we presented an experimental study of intermittent elongated bubbles typical of horizontal plug flows. Bubbles of different shapes and velocities were identified by a hybrid time averaging ultrasonic and high-speed motion visualization techniques. The hybrid ultrasonic technique determines the liquid film thickness under the elongated bubble and liquid plug velocity. The liquid film thickness was obtained by measuring the transit time of an ultrasonic pulse discharged from a single transducer, reflected by the bubble gas-liquid interface and received by the same transducer. The liquid plug velocity was determined by indirect acoustic transmission discharged through the entirely flow cross section by an emitter transducer, reflected by the tube wall and received by a receiver transducer. The high-speed visualization allowed to observe the bubble shape and to measure their velocities. The experimental results have been compared with available empirical correlations. It is concluded that more experimental investigation is needed for the understanding of complex interfacial structure of the horizontal plug flows.

6. Acknowledgements

J.L.H. Faccini is grateful to IAEA for the donation of the instrumentation, and to Silvia B.G. Cesar for technical assistance. P.A.B de Sampaio acknowledges the support of CNPq grant 301045/2003-8. J. Su acknowledges the support of CNPq and FAPERJ.

7. References

Beggs, H. D. and Brill, J. P., 1973, in Hale, C. P., 2000, “Slug Formation, Growth and Collapse”, Ph.D. Thesis, University of London.

Bendicksen, K. H., 1984, “An Experimental Investigation of the Motion of Long Bubbles in Inclined Tubes”, Int. J. Multiphase Flow, Vol. 10, No. 4, pp. 467 - 483.

Chang, J. S., Ichikawa, Y. and Irons G. A., 1982, “Flow Regime Characterization and Liquid Film Thickness Measurement in Horizontal Gas-Liquid Two-Phase Flow by an Ultrasonic Method”, Measurements in Polyphase Flow, Heidrick, T.R., and Patel, B.R., ed., pp. 7 – 12, ASME Press, New York.

Chang, J. S. and Morala, E. C., 1990, “Determination of Two-Phase Interfacial Areas by an Ultrasonic Technique, Nuclear Eng. Design, 122, pp. 143 – 156.

Collier, J. G., 1981, “Convective Boiling and Condensation”, 2nd. Ed., McGraw-Hill Book Company.

Dinh, T. B. and Choi, T. S., 1999, “Application of Image Processing Techniques in Air/Water Two-Phase Flow”, Mechanical Research Communications, Vol. 26, No. 4, pp. 463 – 468.

Fabre, J. and Liné, A., 1992, "Modelling of Two-Phase Slug Flow", Annu. Rev. Fluid Mech., 24, pp. 21– 46.
Faccini, J. L. H., Su, J., Harvel, G. D. and Chang, J. S., 2004, "An Advanced Ultrasonic Technique for Flow and Void Fraction Measurements of Two-Phase Flow", Proceedings of ICONE12, Arlington, Virginia, April 25-29.
Fagundes Netto, J. R., Fabre, J. and Peresson, L., 1999, "Shape of Long Bubbles in Horizontal Slug Flow", Int. J. Multiphase Flow, 25, pp. 1129 – 1160.
Masala, T., Harvel, G. D., Su, J. and Chang, J. S., 2005, "Determination of Interfacial Parameters for Horizontal Two-Phase Intermittent Flow Regimes Using a High Speed Pulse-Echo Ultrasonic Technique", Paper ICONE 13-50600, 13th International Conference on Nuclear Engineering**,** Beijing, China**,** May 16-19.
Mandhane, J. M., Gregory, G. A. and Aziz, K., 1974, "A Flow Pattern Map for Gas-Liquid Flow in Horizontal Pipes", Int. J. Multiphase Flow, 1, pp. 537 – 553.
Nicklin, D. J., Wilkis, J. O. and Davidson, J. F., 1962, in Hale, C. P., 2000, "Slug Formation, Growth and Collapse", Ph.D. Thesis, University of London.
Y. Taitel, A.E. Dukler, Model for predicting flow regime transitions in horizontal and near horizontal gas-liquid flow, AIChE, 22, 591-595, 1976.
Ultraflux – Ultrasonic Measurements, 1998, "MiniSonic 600 and 2000 User's Manual", NT064 ver. B, Ultraflux S.A., Paris, France.
Whalley, P.B., 1996, "Two-Phase Flow and Heat Transfer", Oxford Chemistry Primers, 42, Oxford Science Publications, Oxford.
Wallis, G. B., 1969, "One-dimensional Two-Phase Flow", McGraw Hill Book Company.
Zaruba, A., Krepper, E., Prasser, H. –M. and Reddy Vanga, B. N., 2005, "Experimental Study on Bubble Motion in a Rectangular Bubble Column Using High-Speed Video Observations", Flow Measurement and Instrumentation, 16, pp. 277 – 287.

8. Copyright Notice